2025 23rd European Control Conference (ECC)
June 24-27, 2025. Thessaloniki, Greece

# Nonlinear model predictive control strategies for a cyclorotor wave energy device

Ilias Stasinopoulos, Andrei Ermakov, John V. Ringwood

***Abstract*— Wave energy is one of the untapped renewable energy sources, requiring further development of wave energy converters (WECs) to become competitive with wind and solar energy. A significant challenge for WEC development is the high levelized cost of energy (LCoE) associated with traditional heaving or diffraction-based devices. However, analytical and experimental evaluation of lift-based cyclorotor WECs indicate that these devices can achieve superior power absorption when optimised using advanced control techniques, potentially increasing power production by several times, compared to uncontrolled scenarios. This work presents the first implementation of Nonlinear Model Predictive Control (NMPC) for a cyclorotor WEC. The control strategy relies on the separation principle, assuming accurate wave prediction over the control horizon for panchromatic waves. A comparison of various pitch and/or velocity control strategies is conducted for different irregular sea states. The results, obtained by simulations, confirm and exceed the capability, previously predicted by the theoretical optimal control solution, of a cyclorotor WEC to absorb up to 70% of wave energy.**

## I. Introduction

The European Commission Offshore Renewable Energy (ORE) Strategy [1], released in November 2020, sets a target of achieving 1 GW of ocean energy capacity, including wave and tidal power, by 2030, with an ambitious goal of reaching 40 GW by 2050. Despite the significant potential of ocean wave energy, this energy source remains largely untapped. Traditional wave energy converters (WECs), which harness wave forces through buoyancy or diffraction, have yet to achieve commercial success, due to the high levelized cost of energy (LCoE) [2]. However, recent analytical and experimental studies of lift-force-based cyclorotor WECs [3], conducted as part of the Horizon 2020 LiftWEC project [4], have demonstrated superior power absorption potential, when optimal control strategies are employed [5], [6]. cAdditionally, Atargis Energy Corporation released a progress report, estimating the LCoE for a cycloidal WEC with two hydrofoils to be between 100 and 170 USD/MWh (91-155 EUR/MWh), and sets a target of 60 USD/MWh (55 EUR/MWh) [7], which is competitive with offshore wind.

Cyclorotor WECs (see Fig. 1) offer a variety of potential control actuators [6]. These include slow control inputs, such as structural parameters like rotor radius, submergence depth, and yaw, as well as fast real-time control inputs, including hydrofoil pitch angle and rotational velocity/torque control. The latter variables are particularly critical for maximizing power production.

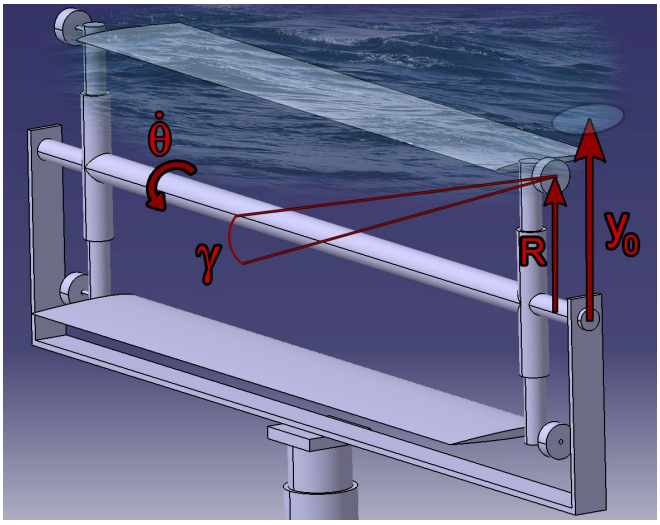


Fig. 1. Concept of a twin-foil cyclorotor wave energy converter, with radius $R$ and submergence depth $y_0$. Fast real-time control inputs include rotational velocity $\dot{\theta}$ and pitch angle $\gamma$.

However, developing a control strategy for cyclorotor WEC devices is a challenging problem, due to the significant non-linearity of the associated mathematical models [8]–[10]. Consequently, most published studies report results obtained using control strategies are mostly for regular waves.

The concept of a 'rotating foil' was first introduced in 1990, demonstrating the capability of a rotating underwater hydrofoil to radiate nearly ideal regular waves [11], [12]. It is noted that this effect can potentially cancel incoming regular waves and absorb their energy. This wave cancellation is achievable if the cyclorotor rotates at the frequency of the incoming waves, with an optimal phase and tuned hydrofoil pitch angle. This analytically and experimentally proven property [13], [14] becomes fundamental to the concept and control strategy of the 'Cycloidal WEC' [15], [16]. The proposed control strategy involves estimating the incoming wave height and period using an up-wave sensor, followed by adjusting the cyclorotor rotational velocity, phase, and pitch, to cancel the wave and absorb its energy [17].

However, more recent research shows that wave cancellation may not be the best metric for assessing the device performance. Instead, evaluating performance based on shaft power is more appropriate [18], [19]. This leads to an alternative control strategy, based on spectral control, which adjusts the pitch and rotational velocity to maximize power

This work was supported in part by a research grant from SFI and the Sustainable Energy Authority of Ireland under SFI-IRC Pathway Programme 22/PATH-S/10793

Authors are with Centre for Ocean Energy Research, Department of Electronic Engineering, Maynooth University, Co. Kildare, Ireland (email: ilias.stasinopoulos.2025@mumail.ie).

generation, assuming ideal knowledge of the relative velocity between the foil and the fluid [5]. It is demonstrated, using this approach, that the cyclorotor must vary the rotational velocity, even in regular monochromatic waves [5], and that simultaneous control of pitch and rotational velocity yields maximum power generation [6]. Another variant of this strategy, applied to a cyclorotor with morphing foils, is proposed in [20]. However, the reported studies [5], [18] are somewhat idealistic in solving the optimal control problem over a complete (long) horizon, with consequently high computational load, and assuming perfect knowledge of the fluid/foil velocity over that timespan.

This paper presents the first application of Nonlinear Model Predictive Control (MPC) for a cyclorotor wave energy converter, which targets shaft power maximisation, but using a realistic receding horizon approach. The control strategy is based on the separation principle, assuming perfect wave induced fluid velocity prediction over the immediate control horizon for panchromatic waves [21]. Different variants of the control strategy are considered, such as pitch-only control, velocity-only control, and combined control. The performance of a cyclorotor WEC under these control strategies is assessed over a period of half an hour, considering various sea states.

The remainder of the article is organised as follows: Section 2 describes a simplified mathematical model for a cyclorotor WEC, which enables receding horizon control implementation. Section 3 introduces the proposed control architecture, including the parametric structure of the performance function, the assumptions of the nonlinear MPC control, along with a description of the selected strategies. Section 4 presents the results, comparing the selected control strategies in terms of wave power absorption. Finally, Section 5 provides the conclusions and discussion.

## II. Mathematical Models

### A. Mathematical model for ocean waves

The cyclorotor WEC is assumed to operate in irregular waves, which are represented by the JONSWAP wave spectrum. This representation allows for a more accurate and realistic modeling of the panchromatic nature of ocean waves. The JONSWAP spectrum is discretized in the frequency domain [22]–[24] and consists of the sum of regular waves, $j$, whose amplitudes, $A_j$, can be calculated as follows:

$$A_j = \sqrt{2S(\omega_j)\Delta\omega}, \tag{1}$$

where $S(\omega_j)$ is the spectral density at frequency $\omega_j$, and $\Delta\omega$ is the frequency discretization step.

The JONSWAP spectrum is defined according to the DNV Environmental Conditions and Environmental Loads Practice Manual [25] as:

$$S_A(\omega_j) = A_\gamma \, S_{PM}(\omega_j) \, \gamma^{\exp\left[-0.5\left(\frac{\omega_j-\omega_p}{\sigma\omega_p}\right)^2\right]}, \tag{2}$$

where $A_\gamma = 1 - 0.287\ln(\gamma)$, $\gamma = 3.3$ is the peak enhancement factor, $\omega_p = 2\pi/T_p$ is the peak wave frequency, $T_p$ is the peak wave period, and the standard deviation $\sigma$ is:

$$\sigma = \begin{cases} 0.07, & \text{if } \omega_j \leqslant \omega_p \\ 0.09, & \text{if } \omega_j > \omega_p \end{cases}. \tag{3}$$

The Pierson-Moskowitz spectrum, $S_{PM}$, in (2) is given by:

$$S_{PM}(\omega_j) = \frac{5}{16} H_s^2 \omega_p^4 \omega_j^{-5} \exp\left[-\frac{5}{4}\left(\frac{\omega_j}{\omega_p}\right)^{-4}\right], \tag{4}$$

where $H_s$ is the significant wave height.

Assuming linear deep-water conditions [26], the wave-induced fluid velocity field for the $j$-th individual wave is computed as:

$$\begin{aligned} w_{x_i,j} &= \frac{\pi A_j}{T_j} e^{k_j y_i} \cos(k_j x_i - \omega_j t + \phi_j), \\ w_{y_i,j} &= \frac{\pi A_j}{T_j} e^{k_j y_i} \sin(k_j x_i - \omega_j t + \phi_j), \end{aligned} \tag{5}$$

where $(x_i, y_i)$ represents the position of the $i$-th hydrofoil underwater, while $A_j$, $k_j$, $\omega_j$, $T_j$, and $\phi_j$ are the amplitude, wave number, angular frequency, period and phase of the $j$-th wave, respectively. The phase $\phi_j$ is drawn from a uniform distribution: $\phi_j \sim \text{Uniform}[0, 2\pi]$. The wave number $k_j$ is computed using the relation $k_j = \omega_j^2/g$ [27], where $g$ is gravitational acceleration.

The total wave-induced fluid velocity components are obtained by summing over all $n$ waves as follows:

$$(V_{W_i})_x = \sum_{j=1}^{n} w_{x_i,j}, \qquad (V_{W_i})_y = \sum_{j=1}^{n} w_{y_i,j}. \tag{6}$$

The power in a typical irregular ocean sea state may be evaluated by:

$$P_{irr} = \frac{1}{64\pi} \rho g^2 H_s^2 T_e, \tag{7}$$

where $\rho = 1000\text{kg/m}^3$ is the water density, and $T_e = \lambda T_p$ is the wave energy period, with $\lambda = 0.8$ representing the proportionality between the peak and energy periods.

### B. Mathematical model for a cyclorotor WEC

This work focuses on a receding horizon control strategy, where minimising computational complexity and execution time is crucial for real-time operation. As a result, the instantaneous radiation and wake effects produced by the moving hydrofoils are neglected [28]. The cyclorotor WEC is modeled using a simplified two-dimensional representation, similar to the approach in [8], [19], [29], where each hydrofoil is treated as a point source. The position $(x_i, y_i)$ of each hydrofoil $i = 1, 2$ is described by:

$$\begin{aligned} x_i(t) &= R\cos\left(\theta(t) + \pi(i-1)\right), \\ y_i(t) &= y_0 - R\sin\left(\theta(t) + \pi(i-1)\right), \end{aligned} \tag{8}$$

where $\theta(t)$ represents the angular position of the hydrofoil in polar coordinates, $R$ is the rotor radius, and $y_0$ is the submergence depth of the rotor center. The rotational velocity

$V_R$ of each hydrofoil is the time derivative of its position, given by:

$$\begin{aligned}(V_{R_i})_x(t) &= -R\,\dot{\theta}\sin\left(\theta(t)+\pi(i-1)\right),\\ (V_{R_i})_y(t) &= -R\,\dot{\theta}\cos\left(\theta(t)+\pi(i-1)\right),\end{aligned} \tag{9}$$

where $\dot{\theta}$ is the angular velocity.

The relative velocity between the hydrofoils and the surrounding fluid is determined by the vector difference between the wave-induced fluid velocity (6) and the hydrofoil rotational velocity (9), expressed as:

$$\hat{\mathbf{V}}_\mathbf{i} = \mathbf{V}_{\mathbf{W_i}} - \mathbf{V}_{\mathbf{R_i}}. \tag{10}$$

The angle of attack for each hydrofoil is calculated as:

$$\alpha_i(t) = \arcsin\left(\frac{(V_{R_i})_x * (\hat{V}_i)_y - (V_{R_i})_y * (\hat{V}_i)_x}{|V_{R_i}||\hat{V}_i|}\right) + \gamma_i, \tag{11}$$

where $\gamma_i$ is the pitch angle of hydrofoil $i$.

Then, the lift and drag forces acting on the rotating hydrofoils can be evaluated as:

$$F_{L_i} = \frac{1}{2}\,S\,C_L(a_i)|\hat{V}_i|^2, \quad F_{D_i} = \frac{1}{2}\,S\,C_D(a_i)|\hat{V}_i|^2, \tag{12}$$

where S is the hydrofoil span, $C_L$ and $C_D$ are the lift and drag coefficients, respectively, which are functions of the angle of attack $a_i$. The lift and drag coefficients are taken from [16], using symmetric hydrofoils NACA0015 [30].

The tangential and radial forces on each hydrofoil $i$ are obtained by projecting the lift and drag forces along the tangential and radial directions of the hydrofoil circular trajectory (see Fig. 2):

$$\begin{aligned}F_{T_i} &= F_{L_i}\sin\left(\alpha_i-\gamma_i\right) - F_{D_i}\cos\left(\alpha_i-\gamma_i\right),\\ F_{R_i} &= F_{L_i}\cos\left(\alpha_i-\gamma_i\right) + F_{D_i}\sin\left(\alpha_i-\gamma_i\right).\end{aligned} \tag{13}$$

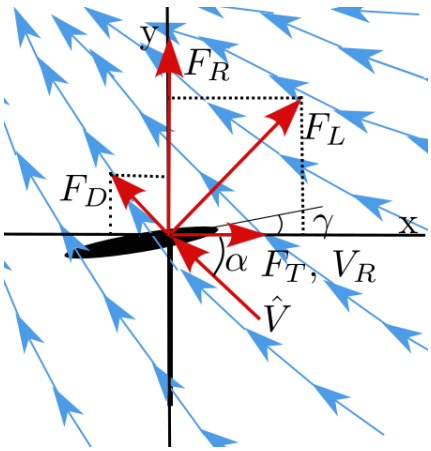


Fig. 2. Interaction between hydrofoil and wave induced velocity.

The tangential components of the lift and drag forces accelerate or decelerate the cyclorotor rotation, generating the wave-induced torque $\mathcal{T}_{Wave}$, which is evaluated as:

$$\mathcal{T}_{Wave} = (F_{T_1} + F_{T_2})R, \tag{14}$$

Wave power is extracted by applying a power take-off (PTO) torque, $\mathcal{T}_{PTO}$. As a result, the dynamics of the controlled cyclorotor are governed by Newton's second law of rotation:

$$I\ddot{\theta}(t) = \mathcal{T}_{Wave} - \mathcal{T}_{PTO}, \tag{15}$$

where I is the inertia of the rotor, $\ddot{\theta}$ is the angular acceleration.

Finally, the average generated mechanical shaft power can be obtained as the time integral of the product of the angular velocity, $\dot{\theta}(t)$, and the PTO torque, $\mathcal{T}_{PTO}$, over the time interval $[0, T]$:

$$P_{Shaft} = \frac{1}{T}\int_0^T \mathcal{T}_{PTO}\dot{\theta}(t)\,dt. \tag{16}$$

The presented integro-differential equations for the mathematical model of ocean waves and a cyclorotor WEC are discretized using the finite-difference method and coded in MATLAB for control implementation.

## III. Control Architecture

The control architecture for a cyclorotor WEC requires the development of an optimal strategy for manipulating the fast control actuators. Adjusting the hydrofoil pitch angles, $\gamma_1$ and $\gamma_2$, ensures the maintenance of the optimal angle of attack. Unlike wind turbines, each hydrofoil in a cyclorotor WEC experiences distinct, wave-induced, fluid velocities. As a result, the optimal pitch angle for each hydrofoil must be evaluated individually. The adjustment of the rotational velocity, $\dot{\theta}$, can be controlled via PTO torque, $\mathcal{T}_{PTO}$. Maintaining the optimal rotational velocity is critical for maximizing shaft power, $P_{Shaft}$, as well as ensuring the optimal angle of attack for each hydrofoil.

The proposed control architecture diagram is presented in Fig. 3. Due to the nonlinear nature of the cyclorotor WEC model, a nonlinear MPC strategy is chosen for actuator manipulation. MPC is an advanced method used to control systems while accounting for system constraints and future behavior by solving an optimization problem based on a specified criterion. MPC was first proposed in the context of wave energy in [31] and, since then, numerous studies have implemented MPC strategies in this field, with variations in the wave energy converter (WEC) model, discretization method, objective function, and optimization algorithm employed [32].

The optimization problem in MPC can include either a performance function based on a reference, or a custom performance function when no reference is available/appropriate. In this case, a custom performance function is used, which balances two conflicting objectives: the maximization of absorbed wave power, and the minimization of structural and PTO loads that can lead to fatigue and damage of the cyclorotor and generator [20]. To address the second objective, a weighted penalty term is introduced to limit large fluctuations in the PTO torque. Thus, the developed performance function has the following form:

$$J = \int_0^{t_p}\left(-P_{Shaft} + \mu\Delta\mathcal{T}_{PTO}^2\right)dt, \tag{17}$$

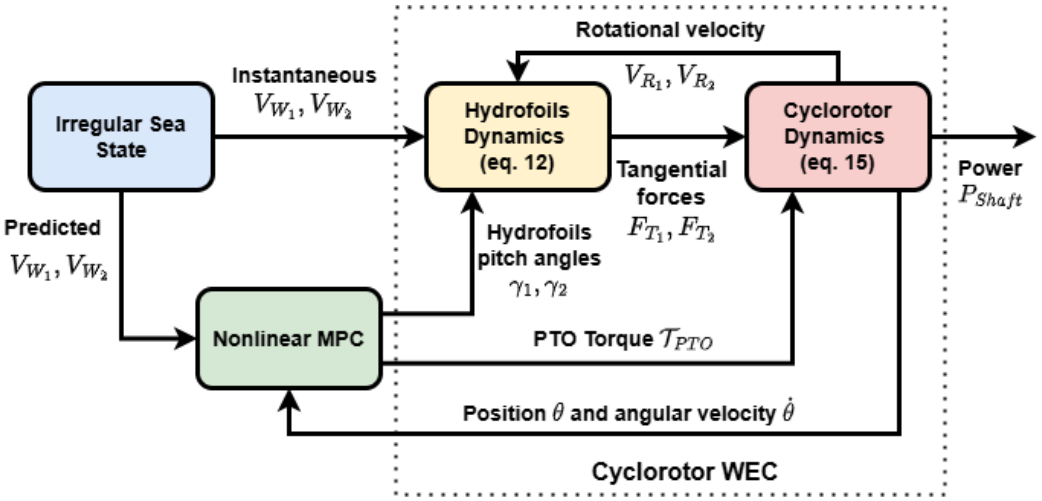


Fig. 3. A control architecture diagram for a cyclorotor WEC

where $t_p$ is the prediction horizon length, $\mu$ is the adjustable weight for the penalty term, and $\Delta\mathcal{T}_{PTO}$ is the maximum change in PTO torque over the time interval $t_p$.

MPC is a receding horizon control method that utilizes a continuously shifting forward prediction horizon to account for the future system behavior. In this context, future information regarding the fluid velocity field $\mathbf{V_W}$ is required. For this study, an ideal state estimator and perfect knowledge of the fluid velocity field within the prediction horizon are assumed, based on the promising results from [28]. This allows the focus to remain solely on control, as outlined by the separation principle proposed in [21].

The structure of the proposed control strategy is as follows (see Fig. 3): Future values of the non-affected by radiation wave-induced fluid velocity $\mathbf{V_W}$ are evaluated using the JONSWAP spectrum (6). Subsequently, the controller solves the optimization problem using the MATLAB 'fmincon' solver, with Sequential Quadratic Programming (SQP) as the optimization algorithm [33]. The performance function, defined in (15), is used to compute the optimal control actions within predefined constraints. These control inputs are then applied to the system, which governs the dynamics of the hydrofoils (12) and the cyclorotor (15). The prediction window is then advanced, and the process is repeated.

The nonlinear MPC is implemented using the MATLAB MPC Toolbox [34], which is capable of handling the high nonlinearity of the system model. This toolbox is previously employed for controlling wave energy converter (WEC) devices by researchers in [35], [36].

## IV. Results

Results are obtained for a cyclorotor similar to the CycWEC concept presented in [16]. The studied cyclorotor has radius $R = 6$m, submergence depth $y_0 = -12$m and two hydrofoils NACA0015 with chord length $C = 5$m, and section mass $m = 1000$kg/m.

The nonlinear MPC requires proper tuning of the prediction horizon length, during which the wave-induced velocity is evaluated. The horizon must be long enough to enable optimal control decisions, but short enough to maintain reasonable computational time. Numerical simulations indicate that a prediction horizon of $t_p = 7.5$ s or even less is sufficient for the chosen cyclorotor WEC concept and the considered nonlinear MPC. Finally, the influence of the weighted penalty term (17) on the system is challenging to be determined analytically, because of the high nonlinearity of the mathematical model. Therefore, is is set to $\mu = 10^{-5}$, empirically, since this value was found to provide the best trade-off between minimising large fluctuations in the PTO torque and maximising mechanical power generation.

Several different sea states, with various wave peak periods $T_p$ and significant wave heights $H_s$, are considered within simulation periods of half an hour each. Three different control strategies, as proposed in [5], [6], are tested:

- The first control strategy - angular velocity control strategy - is based on varying only the angular velocity within the range $(0.2H_s + 0.6)\,\omega_p \leqslant \dot{\theta} \leqslant (0.2H_s + 1)\,\omega_p$ (where $\omega_p = 2\pi/T_p$), while maintaining constant neutral pitch angles, $\gamma_1 = 0$ and $\gamma_2 = 0$.
- The second control strategy - pitch control strategy - involves varying only the hydrofoil pitch angles within the range $-15^\circ \leqslant \{\gamma_1, \gamma_2\} \leqslant 15^\circ$, while keeping a constant angular velocity, $\dot{\theta} = \omega_p$, using PTO torque $\mathcal{T}_{PTO}$.
- The third control strategy - joint pitch and angular velocity control strategy - varies both the angular velocity within $(0.2H_s + 0.6)\,\omega_p \leqslant \dot{\theta} \leqslant (0.2H_s + 1)\,\omega_p$ and the hydrofoil pitch angles within $-15^\circ \leqslant \{\gamma_1, \gamma_2\} \leqslant 15^\circ$.

Results are presented in terms of Capture Width Ratio (CWR) [37], which evaluates wave power extraction in %:

$$CWR = \frac{P_{Shaft}}{P_{irr}} * 100\%. \tag{18}$$

It can be seen, from Table I, which outlines the velocity control strategy, that power absorption increases with the rising of the significant wave height and of the peak period

of irregular waves. The highest power absorption occurs for waves with a peak period of $T_p = 14$ s and significant height $H_s = 5$ m, where a maximum $CWR$ of 20.8% is achieved. However, in most cases involving lower significant wave heights and shorter peak periods, little or no wave power absorption is observed. This is concerning, as such sea states are predominant in many global wave climates.

TABLE I
CWR FOR THE ANGULAR VELOCITY CONTROL STRATEGY IN [%]

| $T_p =$ | 8 s | 10 s | 12 s | 14 s | 16 s |
|---|---|---|---|---|---|
| $H_s = 5$ m | 5.23 | 18.55 | 20.32 | **20.8** | 17.91 |
| $H_s = 4$ m | 0.67 | 13.37 | 18.3 | 13.9 | 15.01 |
| $H_s = 3$ m | 0 | 8.55 | 11.44 | 13.23 | 10.47 |
| $H_s = 2$ m | 0 | 2.36 | 6.51 | 10.01 | 11.68 |
| $H_s = 1$ m | 0 | 0 | 3.09 | 7.42 | 8.19 |

In contrast, the results from the pitch control strategy, presented in Table II, follow a different pattern. The CWR values start relatively high, for smaller wave periods and wave heights, with the exception of $T_p = 8$ s and $H_s = 1$ m, where no wave power absorption is observed. The maximum CWR of 62.24% is achieved at $T_p = 10$ s and $H_s = 1$ m. However, the CWR values decrease progressively as the wave period lengthens and the wave height increases, eventually performing worse than the results for angular velocity control presented in Table I. This behavior can be attributed to the fact that the selected constant rotational velocity, $\dot{\theta} = \omega_p$, may not be optimal for sea states with larger significant wave heights and peak periods, indicating that further optimization of the constant angular velocity is required.

TABLE II
CWR FOR THE PITCH CONTROL STRATEGY IN [%]

| $T_p =$ | 8 s | 10 s | 12 s | 14 s | 16 s |
|---|---|---|---|---|---|
| $H_s = 5$ m | 39.22 | 27.63 | 18.66 | 14.95 | 9.58 |
| $H_s = 4$ m | 40.26 | 37 | 23.94 | 20.08 | 13.21 |
| $H_s = 3$ m | 36.88 | 31.9 | 29.38 | 20.75 | 19.38 |
| $H_s = 2$ m | 39.27 | 52.32 | 38.49 | 34.09 | 23.1 |
| $H_s = 1$ m | 0 | **62.24** | 53.52 | 41.31 | 37.11 |

The optimal control solutions presented in [5], [6] demonstrate superior power production for the joint pitch and velocity control strategy. The results obtained from the nonlinear MPC implementation of this joint control strategy indicate the same. As shown in Table III, the maximum CWR for each sea state is achieved when both angular velocity and pitch angles are controlled, reaching the largest power production of 79.64% CWR for peak period $T_p = 8$ s and significant wave height $H_s = 5$ m. It can be concluded that, under the assumptions of the present model, a full-scale cyclorotor WEC has the potential to offer superior wave energy absorption compared to more traditional WECs [37], if the best control strategy is implemented. However, further studies are required to confirm these findings, including higher-fidelity hydrodynamic modelling and experimental validations.

TABLE III
CWR FOR THE JOINT CONTROL STRATEGY IN [%]

| $T_p =$ | 8 s | 10 s | 12 s | 14 s | 16 s |
|---|---|---|---|---|---|
| $H_s = 5$ m | **79.64** | 68.67 | 54.48 | 38.91 | 29.63 |
| $H_s = 4$ m | 72.83 | 66.4 | 43.5 | 34.74 | 26.55 |
| $H_s = 3$ m | 56.07 | 55.14 | 46.14 | 35.41 | 23.81 |
| $H_s = 2$ m | 45.74 | 65.28 | 43.86 | 36.46 | 28.38 |
| $H_s = 1$ m | 41.07 | 75.83 | 71.45 | 53.89 | 51.52 |

## V. CONCLUSIONS

The tests conducted on the application of nonlinear MPC control for a cyclorotor WEC can be considered successful. The performance assessments, in terms of CWR, are comparable with both analytical model-based performance estimates and optimal control performance evaluations [5], [16], [19]. For example, as estimated in [15], the ability of the cyclorotor to absorb up to 70% of wave power is achieved for specific sea state conditions under the joint control strategy and even outperformed in some cases.

The tests of optimal control strategies for pitch and/or angular velocity, as proposed in [5], [6], demonstrate that the angular velocity control strategy performs better in environments with larger significant wave heights and moderate to high peak wave periods. Conversely, the pitch control strategy performs better in conditions with smaller to moderate significant wave heights and shorter peak wave periods. Finally, the joint control strategy consistently outperforms both individual control strategies across all sea states.

Several factors must be considered when selecting an appropriate control strategy. On one hand, controlling the pitch angle of the hydrofoils appears to be computationally efficient, as it performs well even with a shorter prediction horizon. However, concerns about reliability arise due to the need for continuous pitch adjustments at each time step. The harsh seawater environment can cause wear on pitch actuators, and there is a risk of the hydrofoil becoming locked at an angle unsuitable for optimal power production. On the other hand, angular velocity control is more reliable, as adjustments can be made easily through PTO torque. However, this approach requires a longer prediction horizon to yield effective results, which entails higher computational effort. Additionally, frequent changes in angular velocity may lead to fatigue in the generator or the cyclorotor structure [20].

Finally, controlling both pitch and angular velocity enhances power production but introduces a more complex optimisation challenge. Achieving the global optimum without substantially increasing computational time requires a carefully formulated problem. Thus, further development is required, which will involve testing various optimization solvers, exploring different input constraints, refining performance functions and retuning the prediction horizon length.

Unfortunately, the computational time required for the nonlinear MPC optimization algorithm is currently too long to allow real-time implementation. Additionally, the development of a wave-induced fluid velocity predictor and a

cyclorotor state estimator is necessary for practical real-time control of cyclorotor WECs [28].

Nevertheless, the obtained CWR estimates for the cyclorotor WEC confirm that this device is capable of greater power production compared to more traditional devices [37], when controlled with advanced strategies such MPC. This provides strong motivation for continued research and control development of cyclorotor WECs, which can contribute to the ultimate goal of the commercial viability of the ocean waves as a renewable source of energy.

## REFERENCES


[1] European Commission, *An EU Strategy to Harness the Potential of Offshore Renewable Energy for a Climate Neutral Future*. European Commission, Belgium, 2020.

[2] C. Guo, W. Sheng, D. G. De Silva, and G. Aggidis, "A review of the levelized cost of wave energy based on a techno-economic model," *Energies*, vol. 16, no. 5, 2023.

[3] A. Ermakov and J. V. Ringwood, "Rotors for wave energy conversion—practice and possibilities," *IET Renewable Power Generation*, vol. 15, p. 3091–3108, 2021.

[4] LiftWEC Consortium, https://cordis.europa.eu/project/id/851885/results/ (accessed 08 October 2024), 2024.

[5] A. Ermakov, A. Marie, and J. V. Ringwood, "Optimal control of pitch and rotational velocity for a cyclorotor wave energy device," *IEEE Transactions on Sustainable Energy*, vol. 13, no. 3, pp. 1631–1640, 2022.

[6] J. V. Ringwood and A. Ermakov, "Energy-maximising control philosophy for a cyclorotor wave energy device," in *41st International Conference on Ocean, Offshore & Arctic Engineering (OMAE), Hamburg*, no. 80990. American Society of Mechanical Engineers, 2022.

[7] Atargis Energy Corporation, https://atargis.com// (accessed 17 March 2024), 2024.

[8] A. Ermakov and J. V. Ringwood, "A control-orientated analytical model for a cyclorotor wave energy device with N hydrofoils," *Journal of Ocean Engineering and Marine Energy*, vol. 7, pp. 201–210, 2021.

[9] A. Arredondo-Galeana, G. Olbert, W. Shi, and F. Brennan, "Near wake hydrodynamics and structural design of a single foil cycloidal rotor in regular waves," *Renewable Energy*, vol. 206, pp. 1020–1035, 2023.

[10] P. Lamont-Kane, M. Folley, C. Frost, and T. Whittaker, "Conceptual hydrodynamics of 2 dimensional lift-based wave energy converters," *Ocean Engineering*, vol. 298, p. 117084, 2024.

[11] A. Hermans, E. Van Sabben, and J. Pinkster, "A device to extract energy from water waves," *Applied Ocean Research*, vol. 12, no. 4, pp. 175–179, 1990.

[12] A. Hermans and J. Pinkster, "A rotating wing for the generation of energy from waves," in *Proc. 22nd International Workshop on Water Waves and Floating Bodies*, 2007, pp. 165–168.

[13] S. Siegel, "Wave radiation of a cycloidal wave energy converter," *Applied Ocean Research*, vol. 49, pp. 9–19, 2015.

[14] A. Ermakov, F. Thiebaut, G. S. Payne, and J. V. Ringwood, "Analytical study of pre-stall hydrofoil experimental data for a cyclorotor-based wave energy converter," in *OCEANS 2023 - Limerick, Limerick, Ireland*, 2023, pp. 1–9.

[15] S. Siegel, "Wave climate scatter performance of a cycloidal wave energy converter," *Applied Ocean Research*, vol. 48, pp. 331–343, 2014.

[16] S. G. Siegel, "Numerical benchmarking study of a cycloidal wave energy converter," *Renewable Energy*, vol. 134, pp. 390–405, 2019.

[17] S. Siegel, C. Fagley, and S. Nowlin, "Experimental wave termination in a 2D wave tunnel using a cycloidal wave energy converter," *Applied Ocean Research*, vol. 38, pp. 92–99, 2012.

[18] A. Ermakov, A. Marie, and J. V. Ringwood, "Some fundamental results for cyclorotor wave energy converters for optimum power capture," *IEEE Transactions on Sustainable Energy*, vol. 13, no. 3, pp. 1869–1872, 2022.

[19] A. Ermakov, F. Thiebaut, G. S. Payne, and J. V. Ringwood, "Validation of a control-oriented point vortex model for a cyclorotor-based wave energy device," *Journal of Fluids and Structures*, vol. 119, p. 103875, 2023.

[20] A. Arredondo-Galeana, A. Ermakov, W. Shi, J. V. Ringwood, and F. Brennan, "Optimal control of wave cycloidal rotors with passively morphing foils: An analytical and numerical study," *Marine Structures*, vol. 95, p. 103597, 2024.

[21] D. Bertsekas, *Dynamic Programming and Optimal Control: Volume I*. Athena Scientific, 2012, vol. 4.

[22] T. Jeans, C. Fagley, S. Siegel, and J. Seidel, "Irregular deep ocean wave energy attenuation using a cycloidal wave energy converter," *International Journal of Marine Energy*, vol. 1, pp. 16–32, 2013.

[23] M. L. Jalón and F. Brennan, "Hydrodynamic efficiency versus structural longevity of a fixed OWC wave energy converter," *Ocean Engineering*, vol. 206, p. 107260, 2020.

[24] A. Mérigaud and J. V. Ringwood, "Free-surface time-series generation for wave energy applications," *IEEE Journal of Oceanic Engineering*, vol. 43, pp. 19–35, 2018.

[25] D. N. Veritas, "Recommended practice DNV-RP-C205: environmental conditions and environmental loads," *DNV, Norway*, 2010.

[26] G. B. Airy, *Tides and Waves*. B. Fellowes, 1845.

[27] M. E. McCormick, *Ocean Wave Energy Conversion*. Courier Corporation, 2013.

[28] I. Stasinopoulos, A. M. Ermakov, and J. V. Ringwood, "Relative foil-fluid velocity estimation and forecasting for cyclorotor wave energy conversion," in *Proceeding of IEEE OCEANS 2025 Conference*, Brest, France, June 2025, accepted for publication.

[29] A. Ermakov and J. V. Ringwood, "Development of an analytical model for a cyclorotor wave energy device," in *The 14th European Wave and Tidal Energy Conference, paper #1885, Plymouth, UK*, 2021.

[30] R. E. Sheldahl and P. C. Klimas, *Aerodynamic characteristics of seven symmetrical airfoil sections through 180-degree angle of attack for use in aerodynamic analysis of vertical axis wind turbines*. Sandia National Laboratories, United States, 1981.

[31] P. Gieske, "Model predictive control of a wave energy converter: Archimedes wave swing," 2007.

[32] N. Faedo, S. Olaya, and J. V. Ringwood, "Optimal control, MPC and MPC-like algorithms for wave energy systems: An overview," *IFAC Journal of Systems and Control*, vol. 1, pp. 37–56, 2017.

[33] The Mathworks Inc., "Optimization toolbox version: 24.1 (r2024a)," Natick, Massachusetts, United States, 2024. [Online]. Available: https://www.mathworks.com

[34] The MathWorks Inc., "Model predictive control toolbox version: 24.1 (r2024a)," Natick, Massachusetts, United States, 2024. [Online]. Available: https://www.mathworks.com

[35] M. Richter, M. E. Magana, O. Sawodny, and T. K. A. Brekken, "Nonlinear model predictive control of a point absorber wave energy converter," *IEEE Transactions on Sustainable Energy*, vol. 4, no. 1, pp. 118–126, 2013.

[36] M. Richter, M. E. Magaña, O. Sawodny, and T. K. Brekken, "Power optimisation of a point absorber wave energy converter by means of linear model predictive control," *IET Renewable Power Generation*, vol. 8, no. 2, pp. 203–215, 2014.

[37] A. Babarit, "A database of capture width ratio of wave energy converters," *Renewable Energy*, vol. 80, pp. 610–628, 2015.